[redacted]

NACA

RESEARCH MEMORANDUM

FORCE AND PRESSURE CHARACTERISTICS FOR A SERIES OF NOSE INLETS AT MACH NUMBERS FROM 1.59 TO 1.99

V - ANALYSIS AND COMPARISON ON BASIS OF RAM-JET AIRCRAFT RANGE AND OPERATIONAL CHARACTERISTICS

By E. Howard, R. W. Luidens, and J. L. Allen

Lewis Flight Propulsion Laboratory
Cleveland, Ohio

NATIONAL ADVISORY COMMITTEE
FOR AERONAUTICS

WASHINGTON

September 13, 1951

[redacted]

[redacted]

[redacted]

NATIONAL ADVISORY COMMITTEE FOR AERONAUTICS

RESEARCH MEMORANDUM

FORCE AND PRESSURE CHARACTERISTICS FOR A SERIES OF NOSE INLETS AT MACH NUMBERS FROM 1.59 TO 1.99

V - ANALYSIS AND COMPARISON ON BASIS OF RAM-JET AIRCRAFT RANGE AND OPERATIONAL CHARACTERISTICS

By E. Howard, R. W. Luidens, and J. L. Allen

SUMMARY

Four specific designs of axially symmetric spike-type nose inlets were investigated in the NACA Lewis 8- by 6-foot supersonic wind tunnel at flight Mach numbers from 1.59 to 1.99 and at angles of attack from 0° to 10°. The inlets, designed to operate at a flight Mach number of 1.80, were: an external compression inlet having a relatively blunt or subsonic leading edge (subsonic lip inlet), an isentropic spike inlet having all-external compression (isentropic inlet), an external compression inlet with a relatively sharp lip and low cowl slope (supersonic lip inlet), and an external-internal compression inlet utilizing a perforated cowl (perforated inlet). In this report, the inlets were compared on the basis of the effect of inlet characteristics on ram-jet-engine aircraft range and operational problems. The effects of a burner and exhaust nozzle were analytically added to the experimental cold flow inlet data.

At the design flight Mach number, the maximum aircraft range based on calculated peak engine efficiencies varied 25 percent from the highest value, which indicates the importance of inlet design. The supersonic lip inlet had the highest calculated engine efficiency, the second highest pressure recovery, and the lowest drag of the four inlets investigated. The low drag was associated with a minimum of additive drag (minimum mass spillage) and a low cowl lip angle.

Calculations for a typical supersonic aircraft indicated some increase in range might be obtained from engines utilizing any of the inlets except the perforated inlet if the engine were flown at a moderate angle of attack and the resulting engine lift were utilized.

Evaluation at off-design conditions for an engine optimized for maximum aircraft range (peak engine efficiency) at the design point

[redacted]

indicated that propulsive thrust increased with increasing heat addition in the subcritical flow region in spite of the increasing additive drag. For angles of attack of 3° and 6°, the trends of excess thrust with increasing heat addition were similar to those at 0°. For the perforated inlet, there was a range of total-temperature ratios in the subcritical flow region where, owing to mass spillage through the perforations, increasing the temperature ratio did not yield an increase in propulsive thrust.

Speed stability of a ram-jet-propelled aircraft could be attained with peak engine efficiency at design cruise conditions by means of a fuel flow programmed with flight Mach number for all the inlets except the perforated inlet.

INTRODUCTION

A number of inlet types have been proposed for air-breathing propulsion systems operating at supersonic speeds. One way to evaluate the merits of these inlets is to consider the inlet characteristics in terms of several typical aircraft performance and operational problems. Experimentally determined force and pressure characteristics of a series of typical supersonic inlets designed for a flight Mach number of 1.80 are presented in references 1 to 4. In this report the inlet characteristics presented in the cited references are evaluated at design conditions in terms of the range of a ram-jet-propelled supersonic aircraft. At other than cruise conditions, the inlets are evaluated on the basis of the thrust available for acceleration and maneuvering and with respect to attaining aircraft speed stability.

Four types of axially symmetric spike-type nose inlets were considered: (1) subsonic lip inlet (a conical-spike all-external compression inlet having a relatively blunt or subsonic cowl lip, reference 1); (2) isentropic inlet (an isentropic-spike inlet with all-external compression, reference 2); (3) supersonic lip inlet (a conical-spike all-external compression inlet with a relatively sharp lip and low cowl slope, reference 3); and (4) perforated inlet (a conical-spike external-internal compression inlet with a perforated cowl, reference 4). Force and pressure data were obtained in the NACA Lewis 8- by 6-foot supersonic wind tunnel for flight Mach numbers of 1.59, 1.79, and 1.99, for angles of attack from 0° to 10°, at a Reynolds number of about 3.4×10^6 based on maximum model diameter, and over a range of inlet-flow conditions.

The models were designed for a flight Mach number of 1.80 to yield maximum engine efficiency. The design combustion-chamber Mach number, 0.2, was analytically determined to be optimum for an assumed total-pressure recovery of 0.90 at the design flight Mach number and for an exhaust nozzle with contraction and reexpansion to maximum diameter.

SYMBOLS

The following symbols are used in this report:

a	speed of sound, (ft/sec); or acceleration, (ft/sec^2)
C_D	drag coefficient, D/q_0S
C_{D_e}	external drag coefficient of engine, D_e/q_0S_m
C_{F_n}	net thrust coefficient of engine, F_n/q_0S_m
$C_{F_n}-C_{D_e}$	propulsive thrust coefficient of engine
C_L	lift coefficient, L/q_0S_m
c_p	specific heat for air at constant pressure
D	drag
D_e	force on engine in stream direction determined by applying momentum theorem to air passing outside the engine. (For the perforated inlet, air passing out of perforations is considered passing outside the engine.)
F_n	net force on engine in stream direction determined by applying momentum theorem to air passing through the engine: $\left[\gamma_7 p_7 M_7^2 S_m + (p_7-p_0)\ S_m\right] \cos \alpha - \gamma_0 p_0 M_0^2 S_0$
f/a	fuel-air ratio
g	gravitational constant, (32.2 ft/sec^2)
H	heating value of fuel, (Btu/lb)
J	mechanical equivalent of heat, (778 ft-lb/Btu)
K,k	constants
L	lift, force normal to stream direction
L/D	lift-drag ratio
M	Mach number
P	total pressure

p	static pressure
q	dynamic pressure, $\gamma pM^2/2$
R	range, (ft)
S	area
S_c	inlet capture area, area bounded by circle of diameter equal to cowl lip diameter
S_m	maximum cross-sectional area of engine
S_0	area of free-stream tube that contains mass flow through the engine
S_c/S_m	geometrical characteristic of inlet
S_0/S_m	absolute mass-flow ratio, $\frac{\text{mass flow through engine}}{\rho_0 U_0 S_m}$
T	total temperature, ($^\circ$R)
U	velocity, (ft/sec)
W_f	initial fuel load
w_f	actual fuel rate, (lb/sec)
W_g	initial gross weight
α	angle of attack, (deg)
γ	ratio of specific heats for air
η_c	engine combustion efficiency
η'_e	over-all engine efficiency, $\eta_e\eta_c = \left(\frac{\text{energy output}}{\text{energy input}}\right)$
η_e	engine efficiency parameter, η'_e/η_c
ρ	mass density of air
τ	total-temperature ratio, T_7/T_0

Subscripts:

A	aircraft
a	axial
b	body
e	engine
i	induced
n	normal
s	steady horizontal flight, that is, cruise flight conditions
w	wing
0	free stream
3	combustion-chamber entrance (see fig. 1)
4	immediately after flame holder (see fig. 1)
5	exhaust-nozzle entrance (see fig. 1)
6	exhaust-nozzle throat (see fig. 1)
7	exhaust-nozzle exit (see fig. 1)

METHOD OF ANALYSIS

A simple form of the range relation for supersonic flight at constant speed in the isothermal region of the atmosphere can be written as

$$R = HJ\,\eta'_e \frac{L_{w+b+e}}{D_{w+b}} \log \frac{W_g}{W_g - W_f} \tag{1}$$

In equation (1), range is directly proportional to over-all engine efficiency, which is defined as

$$\eta'_e = \frac{(F_n - D_e)U_0}{HJ\,w_f} \tag{2}$$

The experimental data presented in references 1 to 4 can be more conveniently used if equation (2) is written in the following form, which yields the engine efficiency parameter

$$\eta_e = \frac{\eta'_e}{\eta_c} = \frac{C_{F_n} - C_{D_e}}{S_0/S_m\,(\tau-1)} \left[\frac{M_0^2\, a_0^2}{2gJc_pT_0}\right] \tag{3}$$

(Engine efficiency parameter η_e is hereinafter called engine efficiency.) The bracketed member of equation (3) is constant for a fixed flight Mach number. The thrust is calculated as the exit total momentum (including pressure as well as velocity component of momentum) minus the momentum in the free stream tube entering the engine. For both the thrust and efficiency calculations, the effects of flame-holder pressure loss, heat addition, and nozzle force were analytically determined. The assumed flame-holder loss $\frac{\Delta P_{3-4}}{q_3}$ was 2. One-dimensional flow relations were applied across the heat addition zone (reference 5); the ratio of specific heats of air γ was assumed equal to 1.40 before and 1.30 after heat addition; and the corresponding c_p was 0.264. The converging-diverging exhaust nozzle was assumed to have sonic velocity at the throat, an efficiency of 100 percent, and reexpansion to maximum engine diameter.

The equation used to evaluate the effects of engine lift when the engine is flown at angle of attack can be obtained by rewriting the lift-drag ratio term of equation (1) in the following form where interference effects are neglected.

$$\frac{L_{w+b+e}}{D_{w+b}} = \frac{W_g}{D_b + \left(\frac{1}{L/D}\right)_w (W_g - L_e)} \tag{4}$$

In order to compute the effect of engine lift it was necessary to assume an aircraft configuration which is defined subsequently.

The axial and normal accelerations, presented as an aid in evaluating the magnitude of the excess thrust, are instantaneous values calculated at cruise flight conditions. The axial acceleration was calculated as

$$F_n - D_e = \frac{D_{w+b}}{L_{w+b+e}} W_g + \frac{a_a}{g} W_g \tag{5}$$

The normal acceleration without loss of flight speed was calculated from the relations

$$F_n - D_e = \frac{D_{w+b}}{L_{w+b+e}} W_g + \Delta D_i \tag{6}$$

$$\Delta C_{D_i} = \left(\frac{C_{D_i}}{C_L^2}\right) C_L^2 - C_{D_{i,s}} \tag{7}$$

$$\frac{a_n}{g} = \frac{C_L}{C_{L_s}} \tag{8}$$

RESULTS AND DISCUSSION

Schematic diagrams of the four inlets investigated in references 1 to 4 and the abbreviated nomenclature used for identification are shown in figure 2. The supersonic-lip inlet used herein is designated as inlet B in reference 3. A schematic diagram of a ram-jet engine employing these inlets is shown in figure 1. The exterior of the engine is the same as that of the experimental model.

Experimental force model data necessary for the analysis of these inlets were taken from references 1 to 4 and are presented in figures 3 and 4. The term, critical inlet flow, used herein is the condition of highest pressure recovery in the constant mass-flow (lowest drag) region.

On-Design Evaluation

With engine at zero angle of attack. - At the design Mach number of 1.79, engine efficiency, which is directly proportional to range, is considered as the first criterion for comparing the inlets. The variation of exhaust-nozzle-area ratio (S_6/S_m), propulsive thrust coefficient, and engine efficiency parameter with engine total-temperature ratio is presented in figure 5 for engines utilizing each of the four inlets (references 1 to 4) operating at critical-inlet-flow conditions. (Symbols on curves in fig. 5 indicate the conditions for peak engine efficiency parameter corresponding to optimum exhaust-nozzle-area ratios that were used in subsequent calculations.) Highest efficiency was attained with the supersonic-lip-inlet engine. For the four inlets designed for the same conditions, the calculated peak engine efficiencies varied as much as 25 percent from the highest value which

indicates the importance of inlet design. (When the inlets are compared at total-temperature ratios corresponding to peak engine efficiencies, the propulsive thrust coefficients differ for each inlet. However, aircraft range is proportional to the efficiency if the assumption is accepted that engine size can be adjusted to provide the thrust necessary to propel the aircraft without significantly affecting any of the terms in equation (1), particularly the term involving weight. This assumption is reasonable if the variation in engine weight for the different inlets as compared with aircraft gross weight minus fuel weight is small. For most ram-jet-propelled aircraft configurations, the engine weight is expected to be only a small portion of the aircraft structural weight; thus changes in engine size will result in negligible changes in aircraft weight.)

Comparing the basic data (fig. 3(b)) to the corresponding computed engine performance data (fig. 5) indicates that the supersonic-lip inlet, which had the highest engine efficiency, had the lowest drag of any inlet and almost the highest pressure recovery. The low drag of the inlet is associated with a minimum of additive drag (minimum mass spillage) and low cowl lip slope. The perforated inlet with second highest engine efficiency had the highest pressure recovery, but also a very high drag due to mass spillage through the perforations (even though "normal" shock was downstream of the perforations). The isentropic inlet, which had the lowest total-pressure recovery and highest drag, had the lowest engine efficiency.

With the flame-holder-loss coefficient decreased from 2 to 0, additional computations indicated an increase in absolute efficiency values but no change in the relative order of engine efficiencies. Thus, the relative efficiencies of the inlets appear independent of the initial assumption made for flame-holder loss. Calculations were also made to determine the engine efficiencies at equal combustion-chamber Mach numbers for critical-inlet-flow conditions by estimating the effects of small changes in the ratio S_c/S_m. Results of the calculations indicated small changes in absolute efficiency values but no change in the relative order of engine efficiencies. Also from figure 5 it can be seen that the relative efficiencies at the optimum temperature ratio are indicative of the relative efficiencies for a range of temperature ratios.

With engine at angle of attack. - The effect of angle of attack on the performance of engines with critical-inlet-flow conditions and optimum exhaust nozzles for each angle of attack is shown in figure 6 for the design flight Mach number, 1.79. Efficiency for all engines except the perforated-inlet engine was not appreciably affected up to 3° angle of attack. However, as angle of attack was increased above 3°, engine efficiency was appreciably reduced in all cases. Efficiency

of the supersonic-lip-inlet engine decreased about 38 percent as the angle of attack was raised from 0° to 10°.

The specific inlet characteristics resulting in the decrease in efficiency are shown in figure 4. Although mass flow, pressure recovery, and drag all change, the drag shows the greatest percentage change and is largely responsible for the decrease in engine efficiency with angle of attack. (Increase in drag at angle of attack results primarily from the component of normal force in the drag direction and the normal force arises mainly from the flow over the exterior of the model.)

Although engine efficiency is reduced when the engine is flown at angle of attack, the resulting engine lift may be used to help support the aircraft. The trends of engine total-lift coefficient with angle of attack are shown in figure 7 where total lift is the sum of the external lift presented in references 1 to 4 and the internal lift which results from the momentum change of the air passing through the engine. To evaluate the combined effects of engine lift and efficiency at other than 0° angle of attack, the parameter $\eta_e(L/D)$ from the range relation (equation (1)), where the lift-drag ratio is defined in equation (4), was evaluated for a specific airplane configuration. The airplane design conditions assumed were: flight Mach number, 1.79; altitude, 50,000 feet; airplane initial gross weight, 50,000 pounds; wing lift-drag ratio, 7.16; and body drag, 2300 pounds (corresponding to low-drag body and fuselage density of 30 lb/cu ft). The lift of the body is assumed to be zero. The wing was always considered to be at optimum angle of attack (approximately 4°) and as the angle of attack of the engine was varied the engine size was adjusted so that the propulsive thrust F_n-D_e was equal to the wing plus body drag and the sum of the engine and wing lifts were equal to the gross weight. (Interference effects were neglected.) Thus, as the engine lift increased, the wing size (and hence drag) decreased.

The variation of $\eta_e(L/D)$ with engine angle of attack for the various engines is presented in figure 8. For all except the perforated-inlet engine, some increase in the range parameter $\eta_e(L/D)$ results for small angles of attack. The increase in $\eta_e(L/D)$ with increasing α occurs when the effective aircraft lift-drag ratio $\frac{L_w+L_e}{D_b+D_w}$ increases more rapidly than the engine efficiency decreases. The value of $\eta_e(L/D)$ is always lower at 10° than at 0° angle of attack. (Because the necessary variation of engine size with angle of attack was small, the aircraft structural weight distribution was considered constant; however, the wing weight could be reduced because the required wing size is reduced when part of the wing lift is replaced by engine lift. Therefore, if gross weight is unchanged and additional fuel is carried in

lieu of the portion of wing weight which is eliminated, increases in range over and above those due to increasing the value of $\eta_e(L/D)$ exist.)

Off-Design Considerations

Excess thrust with engine at zero angle of attack. - The excess thrust for maneuver, climb, or acceleration available from an engine optimized for maximum engine efficiency at design cruise conditions can be expressed as the percentage increase in thrust coefficient over that at design cruise conditions as the total-temperature ratio is increased. The results of such calculations are presented in figure 9. The data are presented as a function of total-temperature ratio on the supposition that maximum temperature may be limited by the heating value of the fuel or temperature limits on engine materials. Stoichiometric combustion of octane determined from reference 6 is indicated on appropriate figures. To aid in interpreting the magnitude of the excess thrust available from a fixed geometry engine operating with subcritical inlet flow, the excess thrust for engines with variable exhaust nozzles is also presented. For the supersonic-lip-inlet engine with the exhaust nozzle fixed at optimum and at a total-temperature ratio of 6, the excess thrust available is 31 percent of the design cruise value. This excess thrust corresponds to either an axial acceleration of about 0.05 g or a normal acceleration for maneuver without loss of speed of about 1.4 g (a turning radius of 19 miles) for the typical supersonic airplane previously assumed (initial gross weight, 50,000 lb; altitude, 50,000 ft; $(L/D)_W$, 7.16; and body drag, 2300 lb). If the exhaust nozzle could be adjusted to an area ratio of 1, the excess thrust at a total-temperature ratio of 6 would be about 62 percent of the cruise thrust or double that for the engine with the fixed exhaust nozzle.

Independent of the assumptions necessary to make the calculations presented in figure 9, several general observations may be made concerning the effect of inlet characteristic on the excess thrust available from a ram-jet engine. For all the fixed exhaust-nozzle engines in figure 9 except the perforated-inlet engine, the propulsive thrust increased monotonically with increasing total-temperature ratio even though the additive drag was rising rapidly as the shock moved progressively ahead of the cowl lip (fig. 3(b)). Although the rate of increase in propulsive thrust for a fixed geometry engine is appreciable, it is considerably less than the rate of increase available if critical-inlet-flow conditions (no increase in additive drag) are maintained and a variable-area exhaust nozzle is assumed. (The optimum exhaust-nozzle-area ratio for the isentropic-inlet engine is nearly 1; hence only a small increase in total-temperature ratio is possible before choking in a straight pipe occurs.) For the perforated-inlet engine, it is significant that there is a range of increasing total-temperature ratios

which does not result in an increase in propulsive thrust. This range of total-temperature ratios corresponds to that region of subcritical inlet flow where the rate of drag rise is exceptionally large. This large rate of drag rise is associated with the increasing mass flow which spills through the perforations coincident with the movement of the "normal" shock in the region of the perforations upstream from the diffuser throat towards the cowl lip (fig. 3(b)). With regard to obtaining excess thrust by means which involve subcritical inlet operation, the perforated inlet is the least desirable of the inlets investigated. The other inlets show favorable characteristics.

The solid curves of figure 9 are replotted in figure 10 to present the variation of propulsive thrust coefficient and engine efficiency parameter with combustion-chamber Mach number for ram-jet engines with the exhaust nozzle fixed at the optimum for critical-inlet-flow conditions. From figure 10, the assumption made at the on-design condition that the inlets should be operated at critical-inlet-flow conditions to yield maximum engine efficiencies is justified because, for all the inlets, maximum engine efficiencies are essentially equal to the efficiencies at critical-inlet-flow conditions. In addition, figure 10 is useful for relating the excess thrust characteristics of the inlets to the basic experimental inlet data of figure 3(b), which presents external drag, pressure recovery, and mass flow as a function of combustion-chamber Mach number.

Excess thrust with engine at angle of attack. - In maneuvers requiring excess thrust, such as a turn, the angle of attack of the engine to the air stream differs from the design cruise value; therefore, the excess thrust characteristics of the engines at various engine angles of attack are of interest. Presented in figure 11 is the percentage increase in thrust available above the cruise value at zero angle of attack for a range of temperature ratios and angles of attack. Approximate regions of inlet shock oscillation are indicated for the isentropic and perforated inlets; for the subsonic lip and supersonic lip inlets, shock instability was very slight or not apparent over the range of mass flows corresponding to the total-temperature ratios of figure 11. The 1.4 g normal acceleration estimated in the previous discussion corresponds to an airplane angle of attack increase of approximately 2°. If the engine were designed to operate at zero angle of attack at the cruise condition, the 2° increase in angle of attack for maneuver would not appreciably affect the excess thrust available for any of the engines; at a total-temperature ratio of 6, the reduction of excess thrust for an angle of attack of 2° is about 12 percent of the excess thrust available at 0° for all engines except the perforated-inlet engine.

If the engines were designed to operate at 3° angle of attack (which is indicated in fig. 8 to be desirable for maximum range), an increase in angle of attack of 2° has a greater effect on the excess thrust available from the engine; at a total-temperature ratio of 6, the reduction

in excess thrust for an angle of attack of 5° is about 20 percent of the excess thrust available at 3° for all engines except the perforated-inlet engine.

At 10° angle of attack and a temperature ratio of 6, none of the engines shows an excess of thrust over the cruise value for the engine at zero angle of attack. For the supersonic-lip-inlet and subsonic-lip-inlet engines, the increase in excess thrust with increasing temperature ratio from the value corresponding to critical conditions to 6 remains about the same for each angle of attack. At 10° angle of attack both the perforated-inlet and isentropic-inlet engines show a range of increasing temperature ratios that do not result in an increase in thrust; this may result in part from inlet shock instability.

Speed stability and boost. - The effect of inlet characteristics on the engine performance may influence the ability of the airplane to maintain steady flight at the design Mach number. If the relation between the airplane drag and engine propulsive thrust is such that the forces of the system tend to return the airplane to the design Mach number whenever an externally imposed speed change occurs, the airplane is considered to be speed stable and inherently speed stable if the restoring forces are created without the actuation of controls. Inherent speed stability is more desirable because of its greater simplicity. The degree of speed stability may be represented by a quantity

$$\frac{1}{(C_{F_n}-C_{D_e})}\frac{d\left[(C_{F_n}-C_{D_e})-C_{D_A}\right]}{dM_O}$$

where the terms are evaluated for level flight at the design Mach number and a negative value indicates speed stability.

To study the effect of inlet characteristics on the problem of speed stability, ram-jet engines having the supersonic lip inlet and perforated inlet and designed for peak efficiency at a flight Mach number of 1.79 (discussed previously) are evaluated with respect to two representative aircraft drag curves and for three types of engine fuel-flow control. The general problem studied herein applies to an aircraft in level flight at constant altitude, and with a fixed geometry engine assumed always at zero angle of attack with respect to the air stream. The drag curves considered (at the flight conditions previously specified in the discussion of On-Design Evaluation with engines at angle of attack) are for aircraft with two types of wing:

(1) An unswept wing with a 5-percent biconvex airfoil section

(2) A 60° swept wing and a 5-percent double-wedge airfoil section

The types of fuel flow programming considered are (assuming 100-percent combustion of octane):

(I) Constant fuel-air ratio selected for peak engine efficiency at design cruise conditions

(II) Constant fuel-flow rate selected for peak engine efficiency at design cruise conditions

(III) Fuel flow programmed with flight Mach number defined by linear variation of fuel-air ratio with Mach number about the design point,

$$\frac{d(f/a)}{dM_O} = K$$

such that

$$\frac{\left[(C_{F_n}-C_{D_e})-C_{D_A}\right]_{M_O=1.74}}{(C_{F_n}-C_{D_e})_{M_O=1.79}^{(1.79-1.74)}} = k = -1.0$$

and limited by an upper limit of stoichiometric fuel-air ratio f/a of 0.067; (the corresponding total-temperature ratio was determined from data of reference 6) and a lower limit of f/a of 0.01. The fuel-air ratio at the design Mach number provides peak engine efficiency.

The discussion is limited to the underspeed condition where subcritical inlet operation is required and the inlet characteristics are essentially involved. (The overspeed condition involves supercritical inlet operation and the inlet performance is not significant; however, the overspeed condition is included in fig. 12. From fig. 12, the type of control which yields underspeed speed stability will apparently yield overspeed speed stability.) In figure 12(a), two airplane drag coefficient curves and the engine propulsive thrust coefficient curves of the supersonic lip inlet for the three types of fuel control considered are presented. The simple types of fuel control, I and II, yield speed instability or a small degree of speed stability about the design point A depending on the airplane drag characteristics. With fuel control III illustrated with the unswept wing airplane, any desired degree of speed stability is attainable. The subsonic lip inlet and isentropic inlet have similar characteristics.

The propulsive thrust characteristics of the perforated inlet for the three types of fuel control considered are compared with the same drag curves and presented in figure 12(b). Both simple types of fuel control, I and II, demonstrate speed instability about design point A and markedly so for Mach number increments of the order of 0.1. (Inlet characteristics were experimentally determined at only three Mach numbers; however, from these data and the geometrical characteristics of the inlet, estimating the type of performance to be expected at the intervening Mach numbers is possible.) Figure 13 presents the engine propulsive thrust coefficients as a function of total-temperature ratio for three flight Mach numbers for the perforated lip inlet as contrasted with the supersonic lip inlet. (The discontinuous decrease in thrust with decreasing Mach number (point B) occurs at the Mach number where choking occurs at the inlet throat. The precise Mach number at which the discontinuity occurs will depend on the particular design.) Even with the programmed fuel flow (type III), speed instability exists about point A because of two perforated-inlet characteristics: (1) the thrust of the engine does not increase with increasing fuel flow when the "normal" shock is in the region of the perforations and (2) the thrust of the engine decreases with decreasing Mach number when the shock is in the region of the perforations (fig. 13). A speed stable point does exist at point C (fig. 12(b)); however, at this condition the engine efficiency is greatly reduced from its value at the design Mach number (point A) because the "normal" shock is ahead of the inlet and a corresponding high drag exists.

Any engine can probably be made to yield speed stability either (1) with a programmed fuel flow and operating the inlet supercritically at the design Mach number and critically at a lower Mach number or (2) by simultaneously varying the exhaust-nozzle size and the fuel flow. The first method necessitates a decrease in efficiency over the maximum possible at the design Mach number, whereas the second results in a continuously hunting system and considerable mechanical complexity.

Speed stability of a ram-jet-propelled aircraft utilizing a fixed geometry engine with peak engine efficiency at design cruise conditions could be attained for all the inlets except the perforated inlet by means of a fuel flow programmed with flight Mach number.

The lowest Mach number at which the thrust exceeds the drag (fig. 12, point D) is the minimum Mach number to which the aircraft must be boosted before it can accelerate itself to the design Mach number. The calculations of figure 12 were made for the design altitude. The perforated inlet must be boosted to a higher Mach number than the supersonic lip inlet assuming a fixed exhaust-nozzle engine.

CONCLUDING REMARKS

Force and pressure data obtained in the NACA Lewis 8- by 6-foot supersonic tunnel at flight Mach numbers of 1.59, 1.79, and 1.99 and angles of attack from 0 to 10° for a series of axially symmetric nose inlets were analyzed. The inlets, a subsonic lip inlet, an isentropic inlet, a supersonic lip inlet, and a perforated inlet, were compared on the basis of ram-jet-propelled aircraft range and operational characteristics. Effects of a burner and a converging-diverging sonic throat exhaust nozzle reexpanding to maximum body diameter were analytically added to the experimental cold flow inlet data. Inlets considered herein were specific designs and do not necessarily represent optima of their types.

1. The inlet which yielded the highest calculated engine efficiency was characterized by the next to the highest pressure recovery and the lowest drag. The low drag of the inlet was associated with a minimum of additive drag (minimum mass spillage) and a low cowl lip angle.

2. For the four inlets designed for maximum efficiency the maximum aircraft range based on peak engine efficiencies calculated from experimental results varied 25 percent from the highest value, which indicates the importance of inlet design.

3. Calculations for a typical supersonic aircraft indicated that some increase in range might be obtained from engines utilizing any of the inlets except the perforated inlet if the engine were flown at a moderate angle of attack and the resulting engine lift were utilized.

4. For all inlets the propulsive thrust increased with increasing heat addition in the subcritical flow region in spite of the increasing additive drag. For the perforated inlet there was a range of temperature ratios in the subcritical flow region where owing to mass spillage through the perforations increasing the temperature ratio did not yield an increase in propulsive thrust. For angles of attack of 3° and 6°, the trends of excess thrust with increasing heat addition were similar to those at 0°.

5. Fixed geometry engines utilizing any of the inlets except the perforated inlet could be made speed stable while maintaining peak efficiency at the cruise condition by means of a fuel flow programmed with flight Mach number.

Lewis Flight Propulsion Laboratory
National Advisory Committee for Aeronautics
Cleveland, Ohio

REFERENCES

1. Esenwein, Fred T., and Valerino, Alfred S.: Force and Pressure Characteristics for a Series of Nose Inlets at Mach Numbers from 1.59 to 1.99. I - Conical-Spike All-External Compression Inlet with Subsonic Cowl Lip. NACA RM E50J26, 1950.

2. Obery, L. J., and Englert, G. W.: Force and Pressure Characteristics for a Series of Nose Inlets at Mach Numbers from 1.59 to 1.99. II - Isentropic-Spike All-External Compression Inlet. NACA RM E50J26a, 1950.

3. Weinstein, Maynard I., and Davids, Joseph: Force and Pressure Characteristics for a Series of Nose Inlets at Mach Numbers from 1.59 to 1.99. III - Conical-Spike All-External Compression Inlet with Supersonic Cowl Lip. NACA RM E50J30, 1950.

4. Madden, Robert T., and Kremzier, Emil J.: Force and Pressure Characteristics for a Series of Nose Inlets at Mach Numbers from 1.59 to 1.99. IV - Conical-Spike External-Internal Compression Inlet Utilizing Perforated Cowl. NACA RM E51B05, 1951.

5. Bailey, Neil P.: The Thermodynamics of Air at High Velocities. Jour. Aero. Sci., vol. 11, no. 3, July 1944, pp. 227-238.

6. Williams, Glenn C., and Quinn, John C.: Ram Jet Power Plants. Jet Propelled Missiles Panel, OSRD, May 1945. (Under Assignment to Coordinator of Research and Development, U. S. Navy.)

[redacted]

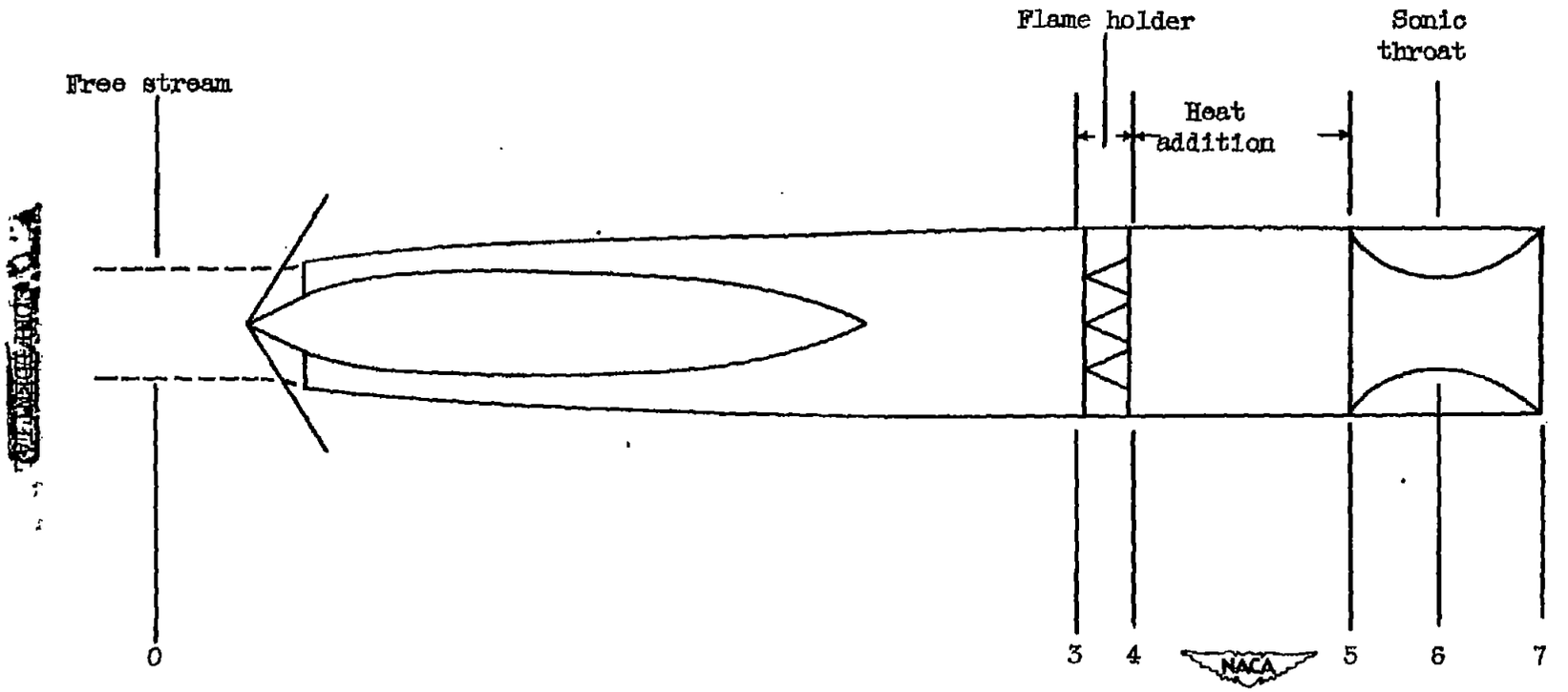

Figure 1. - Ram-jet-engine configuration used in analysis of inlet data.

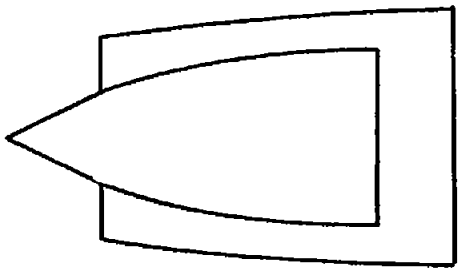

(a) Conical-spike all-external compression inlet with a subsonic cowl lip (subsonic lip inlet).

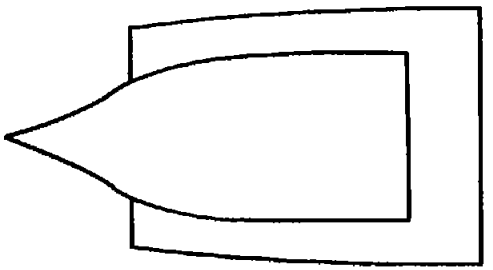

(b) Isentropic-spike all-external compression inlet (isentropic inlet).

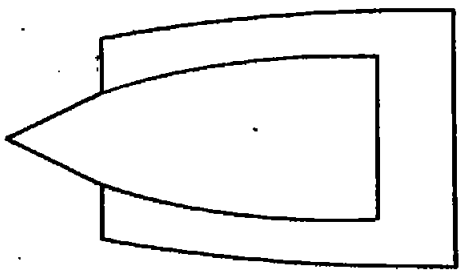

(c) Conical-spike all-external compression inlet with a supersonic cowl lip (supersonic lip inlet).

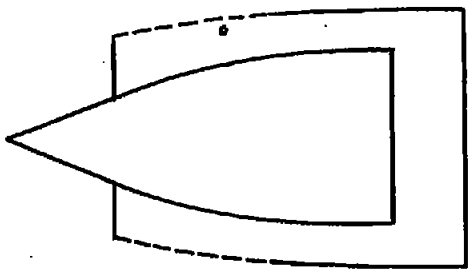

(d) Conical-spike external - internal compression utilizing a perforated cowl (perforated inlet).

Figure 2. - Schematic diagrams of four inlets previously investigated (references 1 to 4). (Abbreviated nomenclature in parentheses is used throughout the present report.)

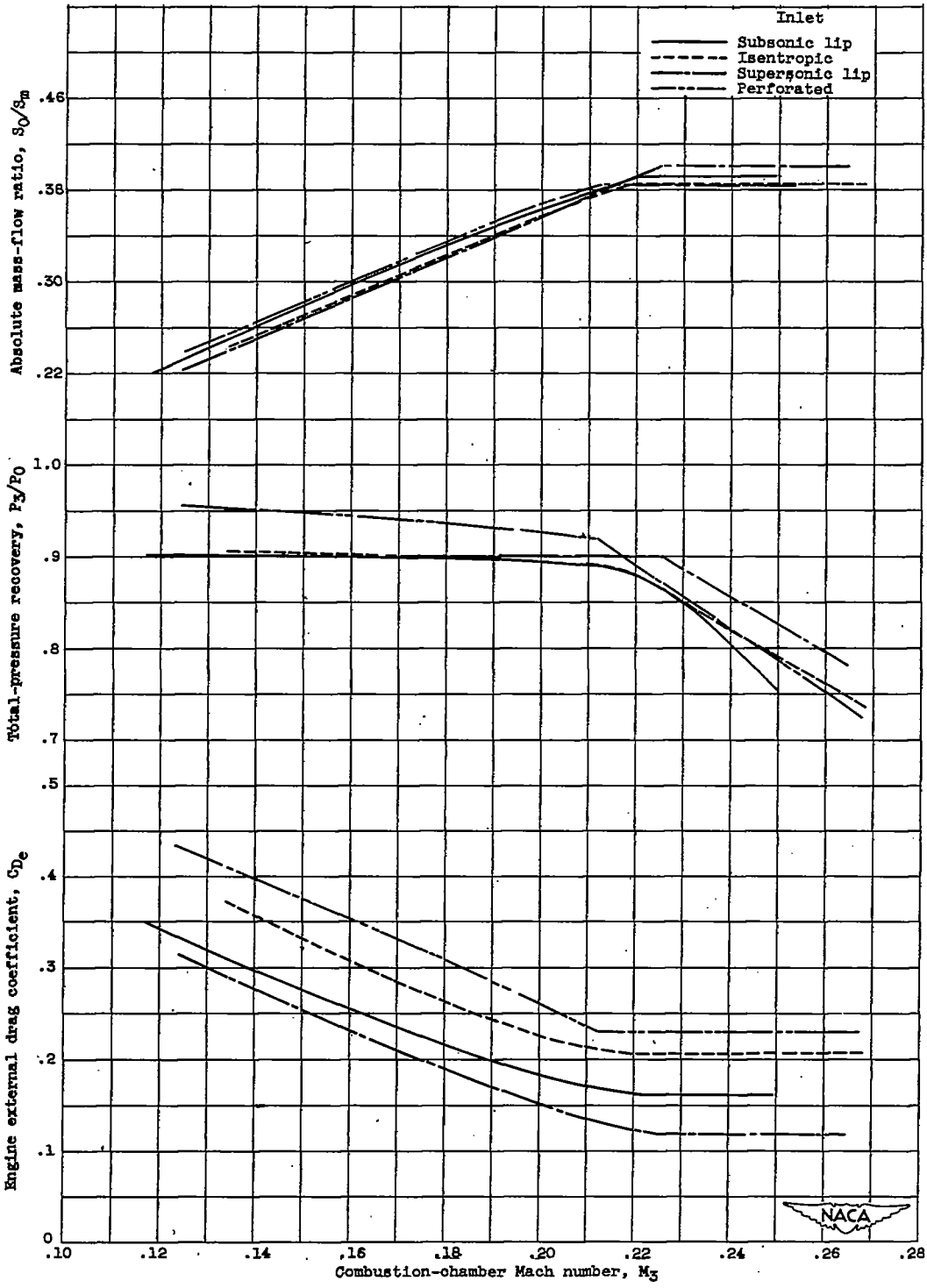

(a) Flight Mach number, 1.59.

Figure 3. - Variation of basic inlet data with combustion-chamber Mach number from references 1 to 4. Angle of attack, 0°.

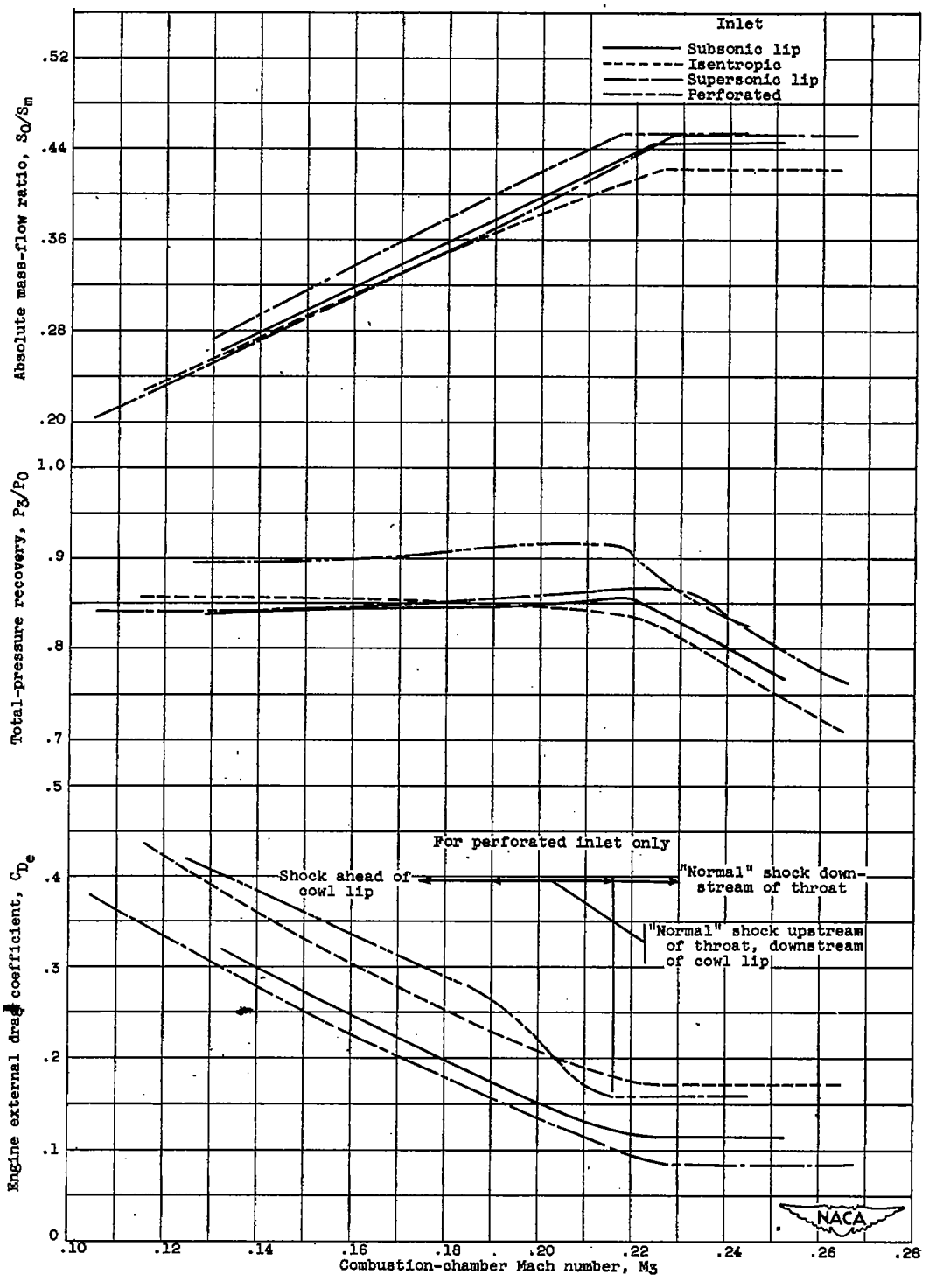

(b) Flight Mach number, 1.79.

Figure 3. - Continued. Variation of basic inlet data with combustion-chamber Mach number from references 1 to 4. Angle of attack, 0°.

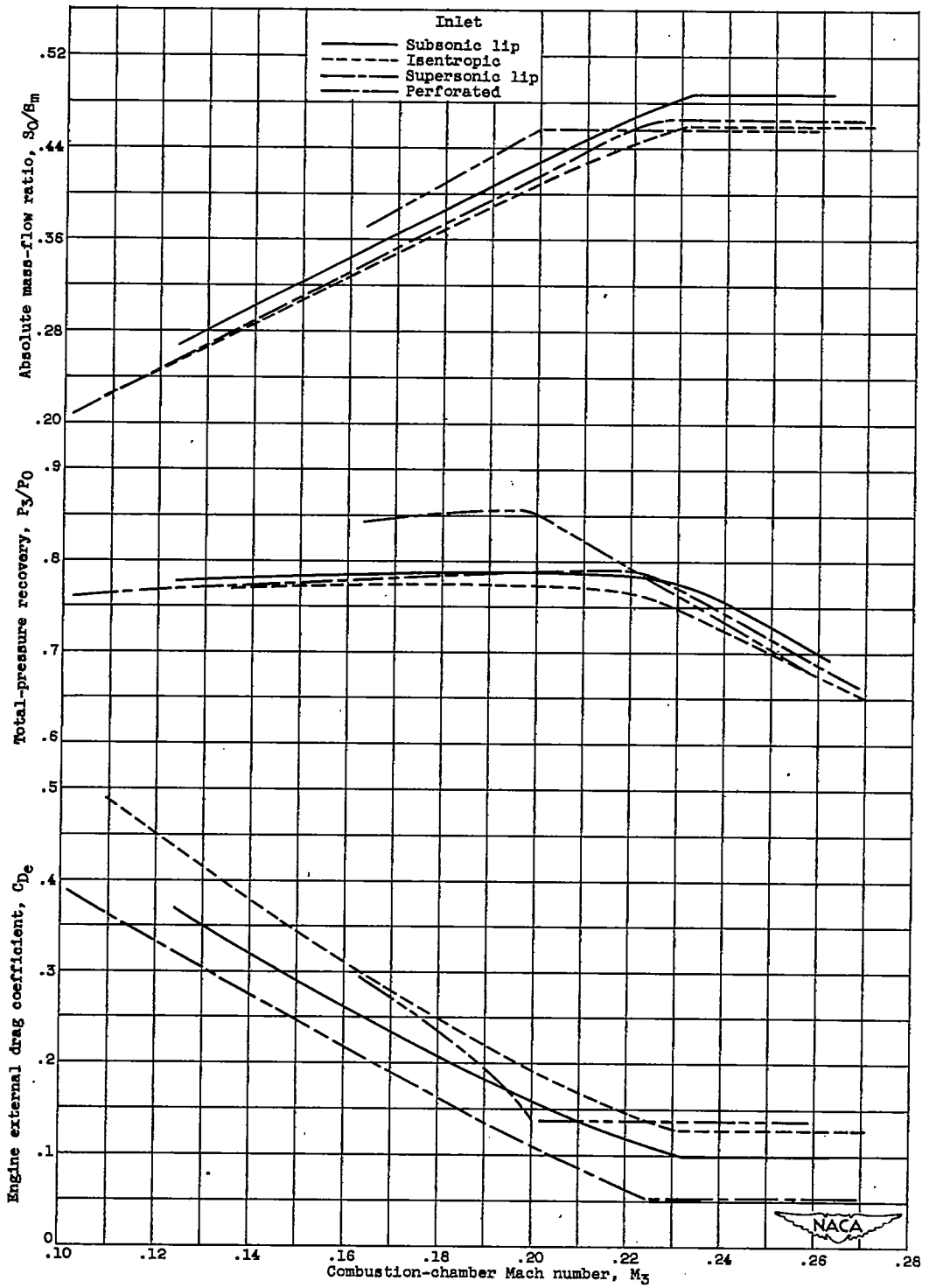

(c) Flight Mach number, 1.99.

Figure 3. - Concluded. Variation of basic inlet data with combustion-chamber Mach number from references 1 to 4. Angle of attack, 0°.

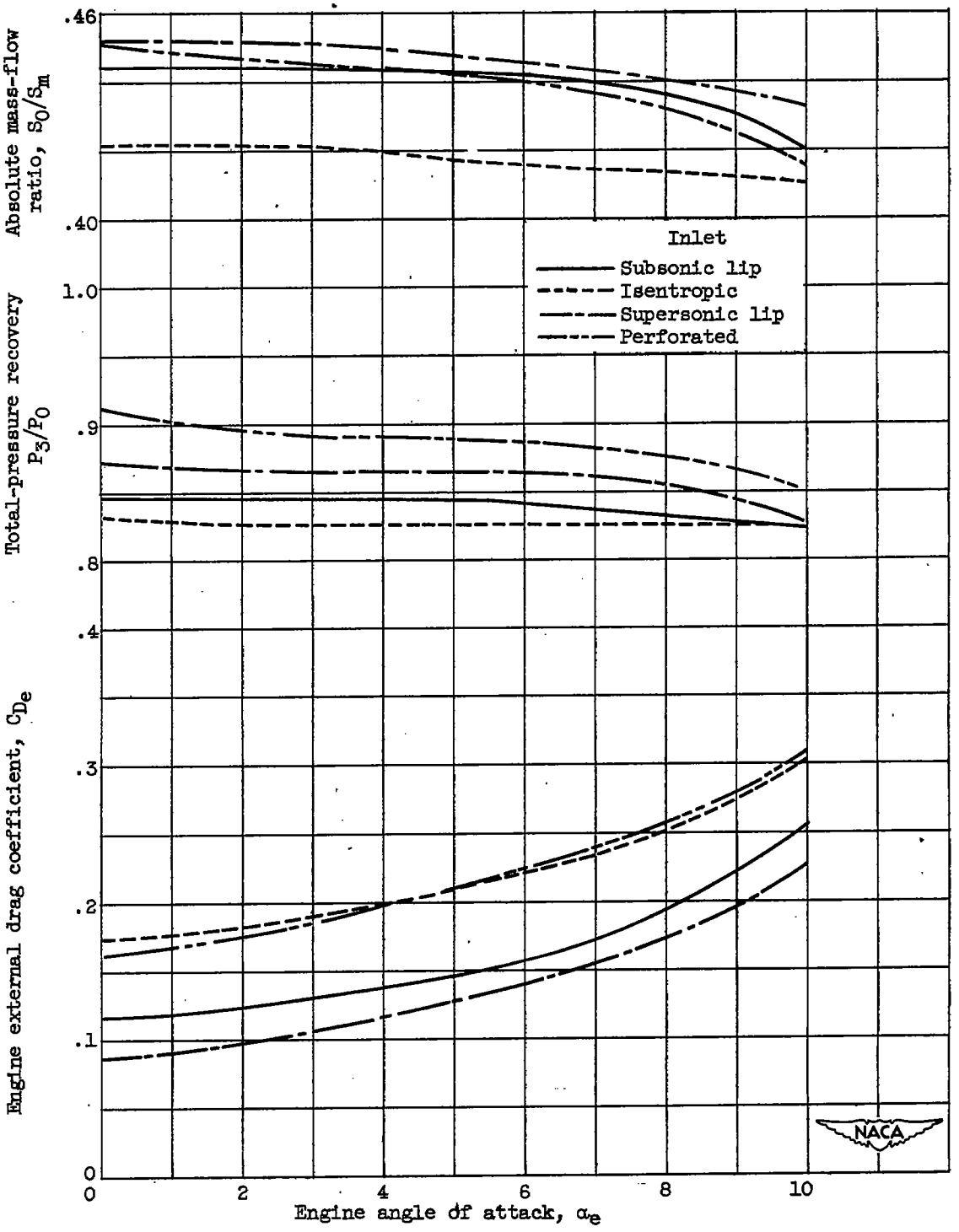

Figure 4. - Variation of basic inlet data with engine angle of attack from references 1 to 4. Critical-inlet-flow conditions at each angle of attack; flight Mach number, 1.79.

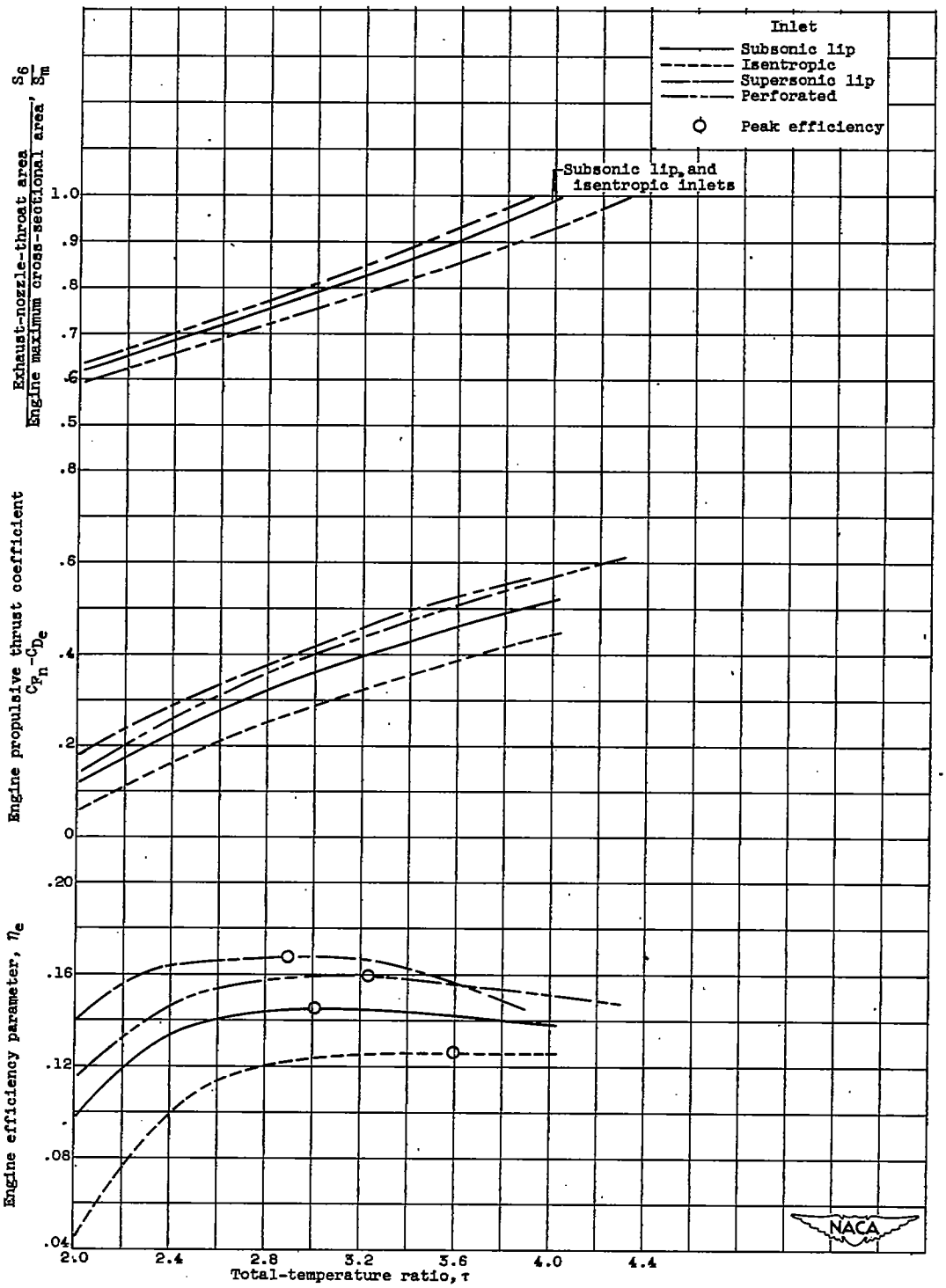

Figure 5. - Variation of engine efficiency parameter, propulsive thrust coefficient, and exhaust-nozzle-area ratio with total-temperature ratio for the four types of inlets at flight Mach number of 1.79. Critical-inlet-flow conditions; angle of attack, 0°.

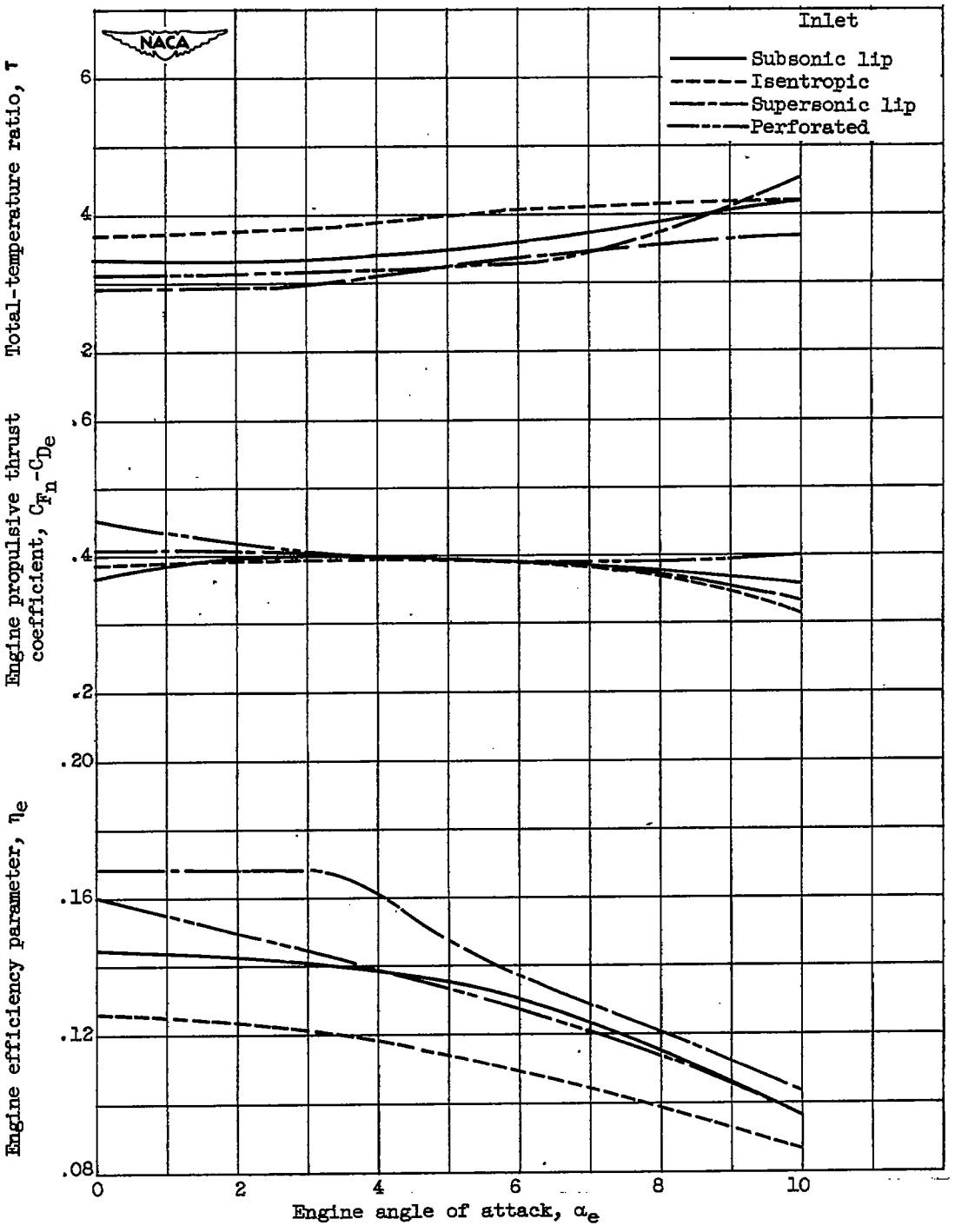

Figure 6. - Variation of engine efficiency parameter, propulsive thrust coefficient, and total-temperature ratio for the four inlets with engine angle of attack. Critical-inlet-flow conditions; optimum exhaust-nozzle-area ratio (peak engine efficiency) for each engine at each angle of attack; flight Mach number, 1.79.

[redacted]

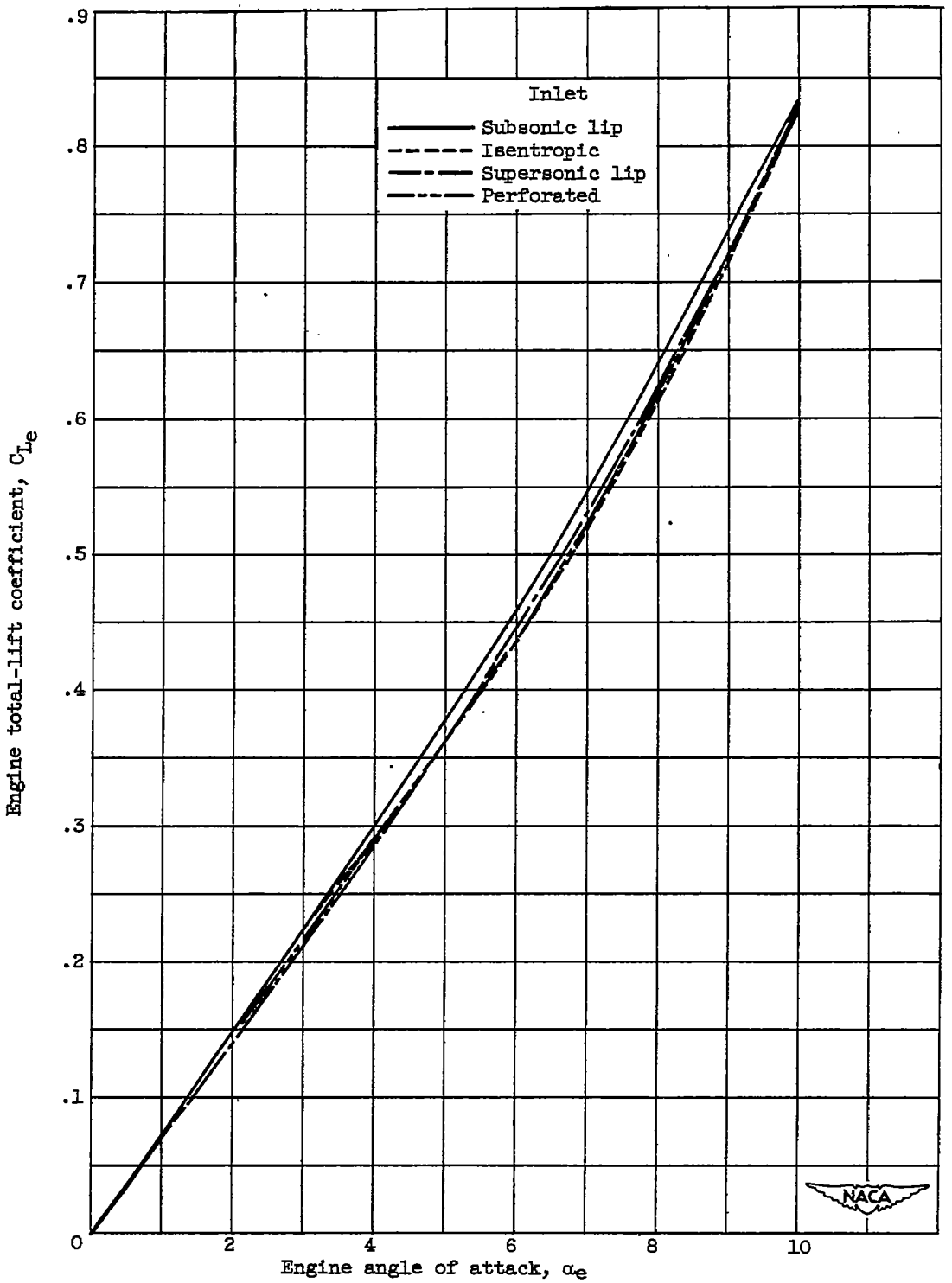

Figure 7. - Variation of engine total-lift coefficient (external plus internal lift) with engine angle of attack. Critical-inlet-flow conditions at each angle; flight Mach number, 1.79.

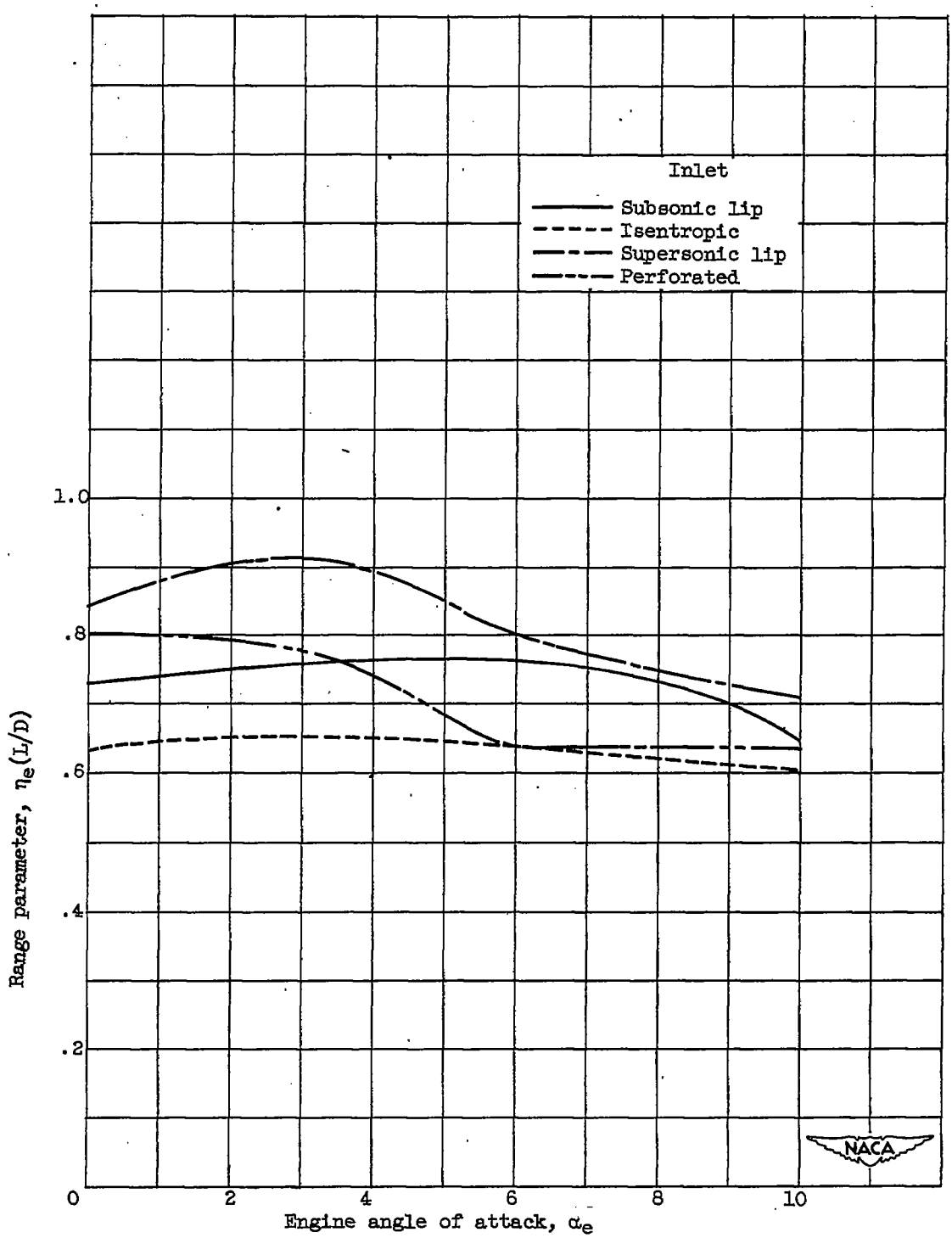

Figure 8. - Variation of range parameter with engine angle of attack as engine lift is utilized instead of wing lift. Optimum exhaust-nozzle-area ratio and critical-inlet-flow conditions for each engine at each angle; flight Mach number, 1.79.

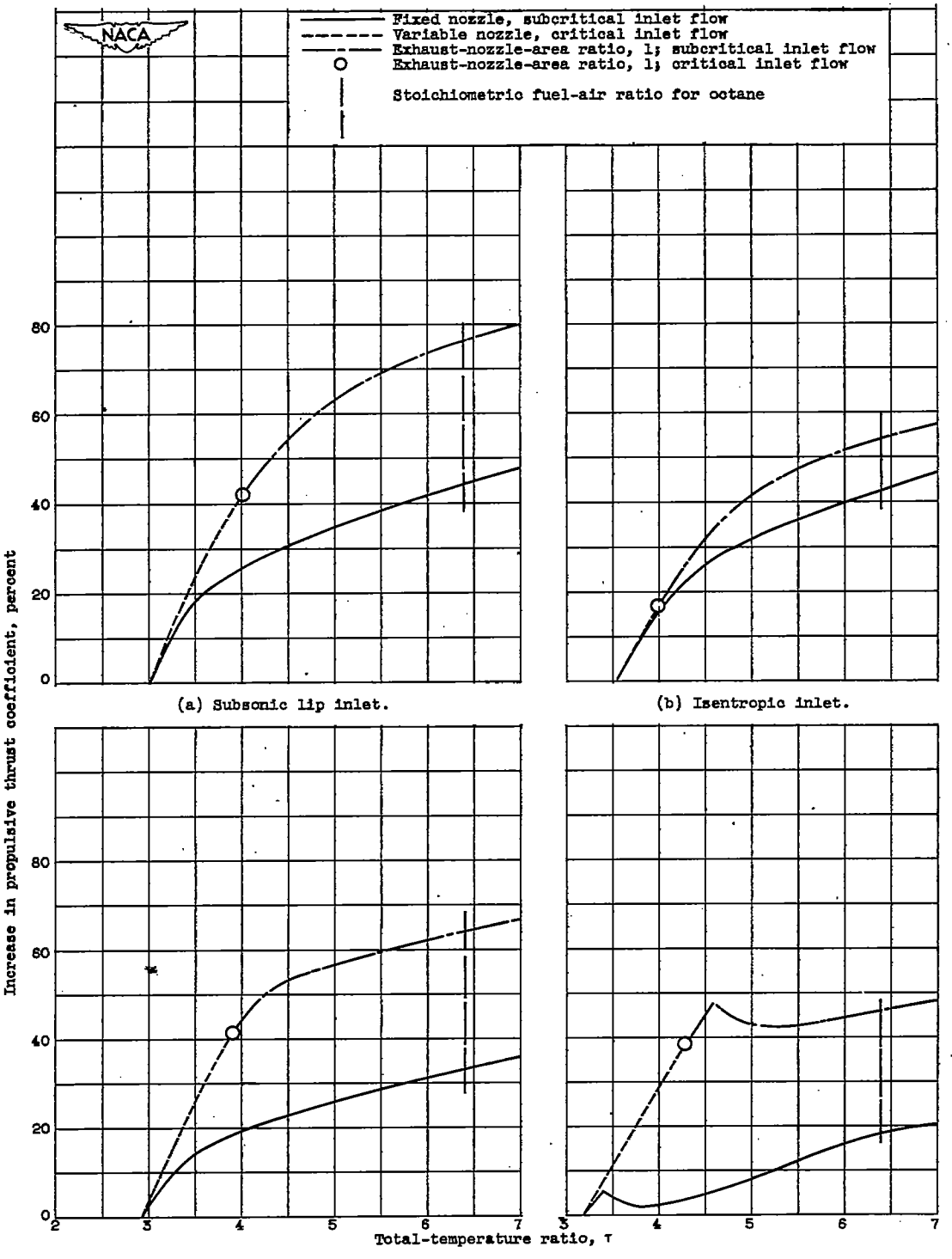

Figure 9. - Variation of percentage increase in propulsive thrust coefficient over that for peak engine efficiency with total-temperature ratio for engines with variable exhaust-nozzle-area ratio and exhaust-nozzle-area ratio fixed for peak efficiency at critical-inlet-flow conditions. Angle of attack, 0°; flight Mach number, 1.79.

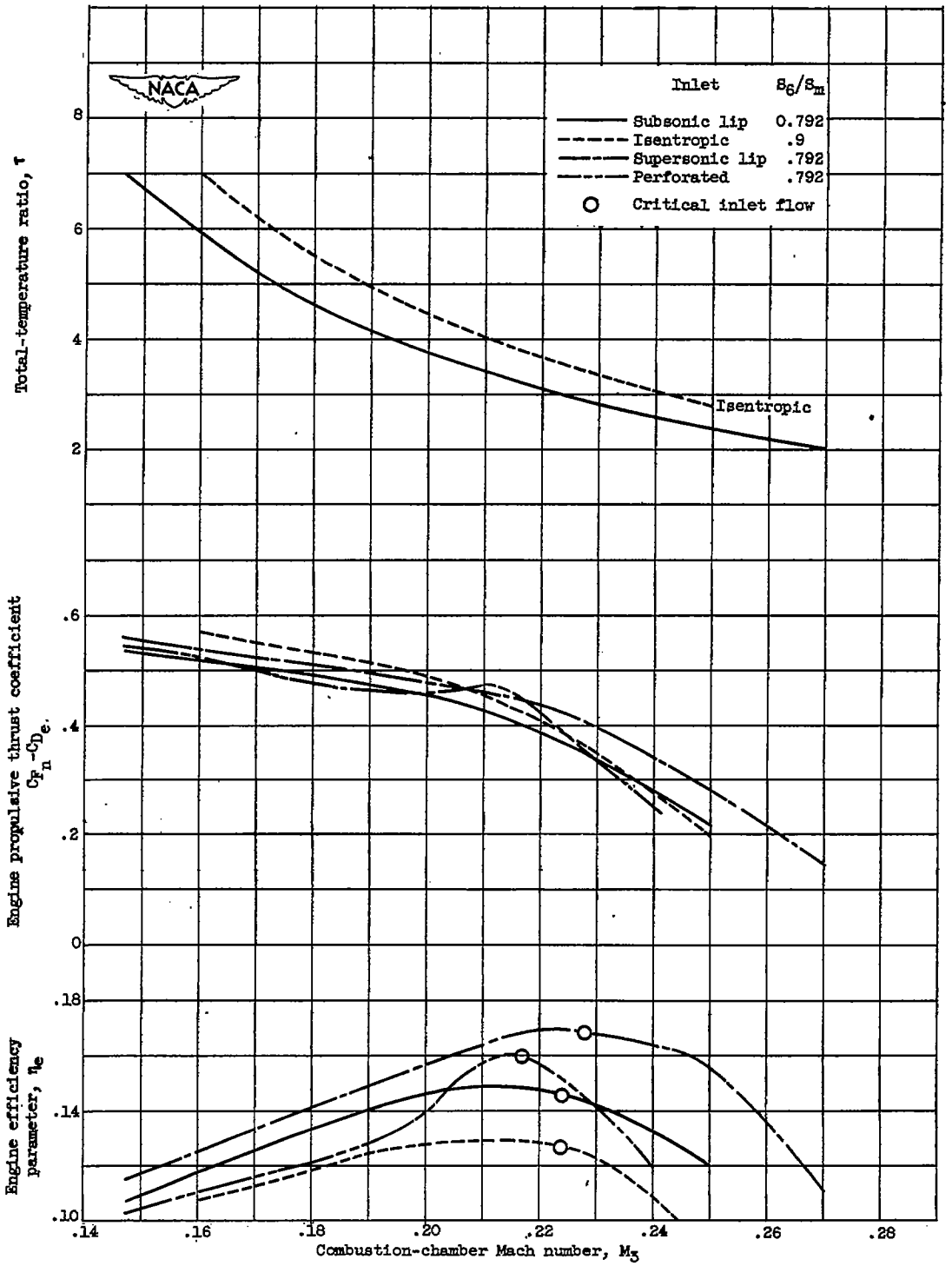

Figure 10. - Variation of engine efficiency, propulsive thrust coefficient, and total-temperature ratio with combustion-chamber Mach number for four inlets. Exhaust-nozzle-area ratio fixed for peak efficiency at critical-inlet-flow conditions. Engine angle of attack, 0°; flight Mach number, 1.79.

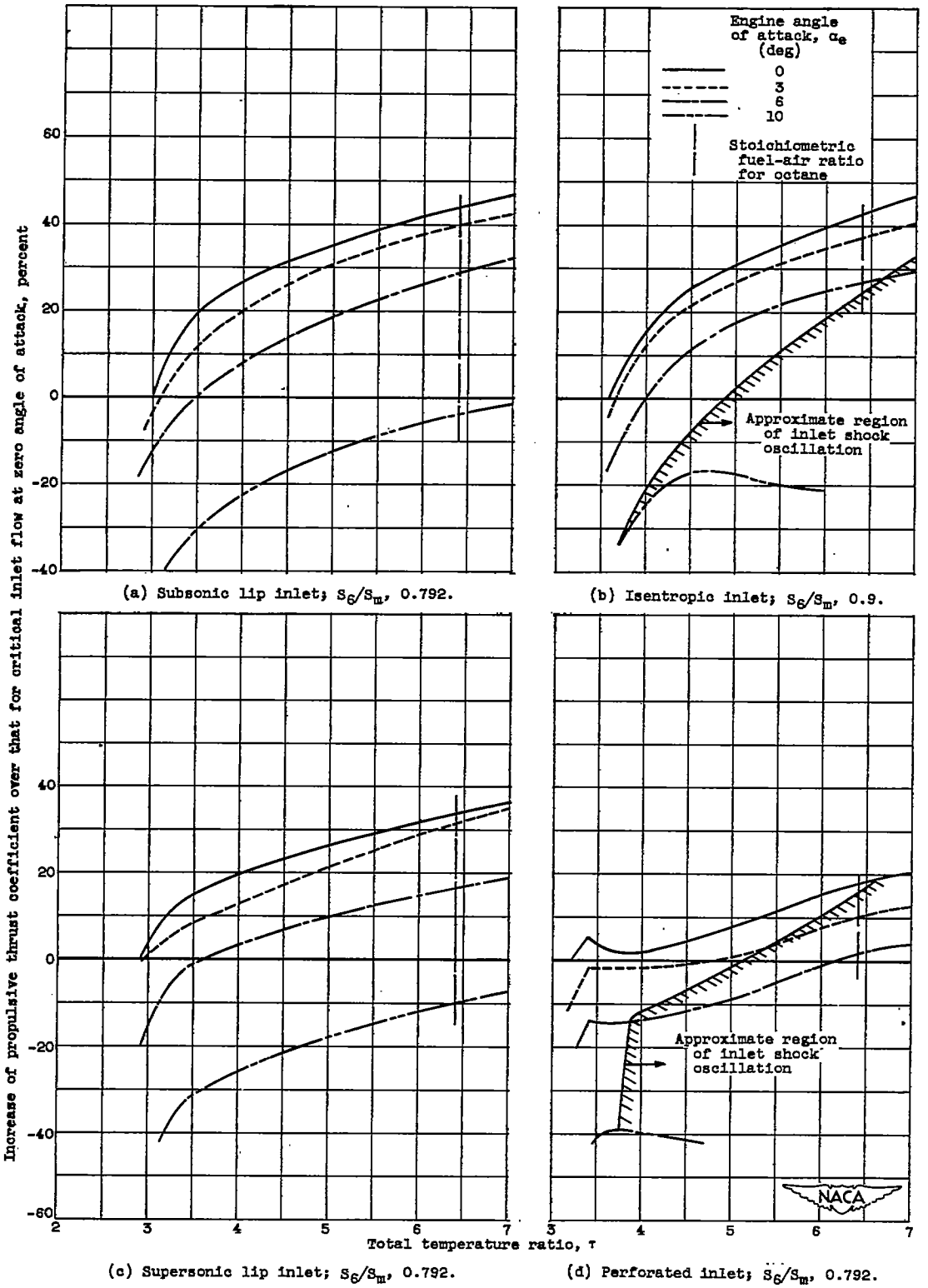

(a) Subsonic lip inlet; S_6/S_m, 0.792.

(b) Isentropic inlet; S_6/S_m, 0.9.

(c) Supersonic lip inlet; S_6/S_m, 0.792.

(d) Perforated inlet; S_6/S_m, 0.792.

Figure 11. - Variation of percentage increase of propulsive thrust coefficient over that for peak efficiency at zero angle of attack with total-temperature ratio for several angles of attack. Flight Mach number, 1.79; exhaust-nozzle-area ratio fixed for peak efficiency at critical-inlet-flow conditions at zero angle of attack.

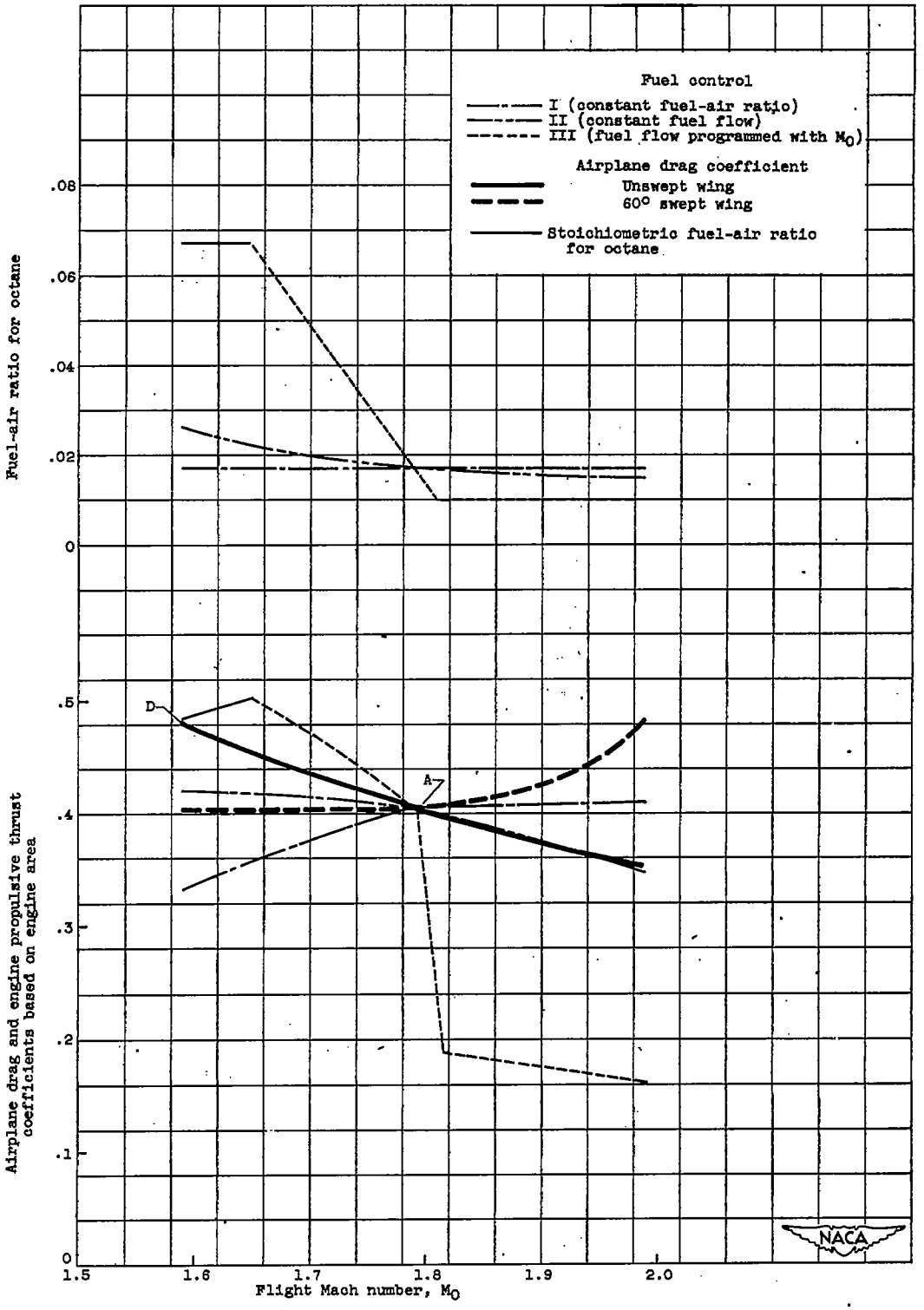

(a) Supersonic-lip-inlet engine.

Figure 12. - Speed stability characteristics for airplane with unswept wing or with 60° swept wing and various types of fuel control.

[redacted]

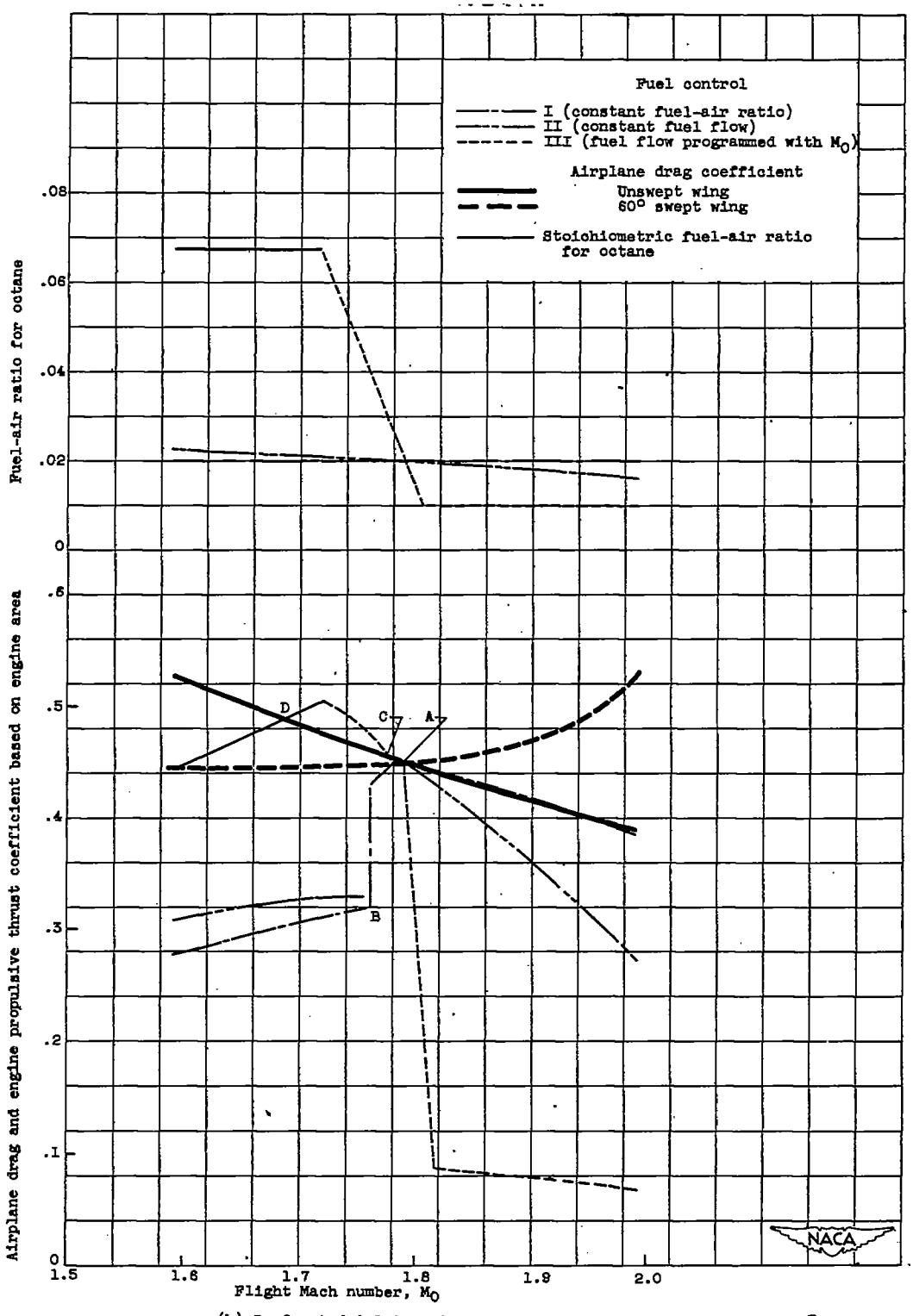

(b) Perforated-inlet engine.

Figure 12. - Concluded. Speed stability characteristics for airplane with unswept wing or with 60° swept wing and various types of fuel control.

[redacted]

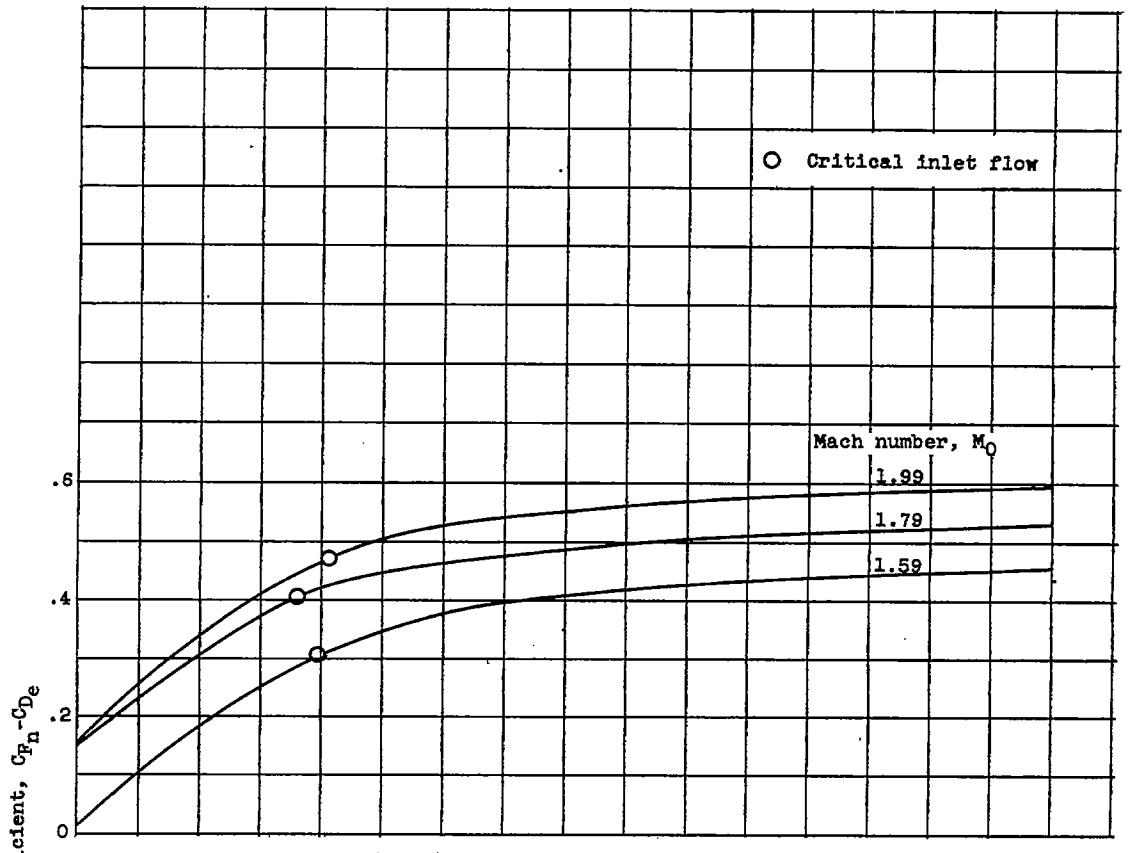

(a) Supersonic-lip-inlet engine.

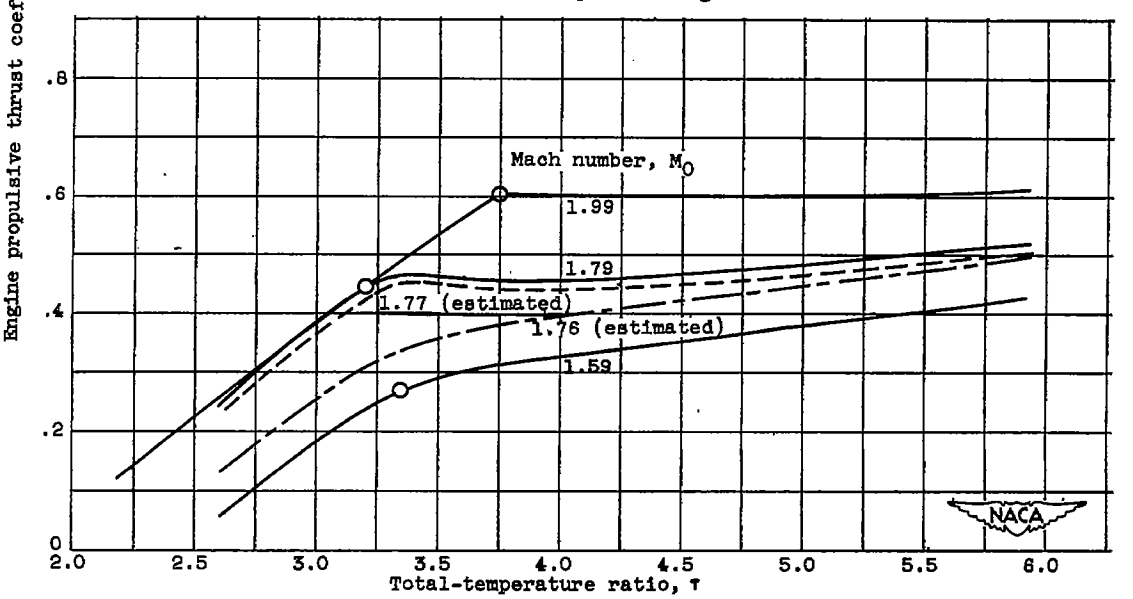

(b) Perforated-inlet engine.

Figure 13. - Variation of engine propulsive thrust coefficient with flight Mach number and total-temperature ratio for supersonic lip and perforated inlets. Optimum exhaust-nozzle-area ratio for design cruise conditions; engine angle of attack, 0°.

[redacted]